Hydration dynamics in water clusters via quantum molecular dynamics simulations

László Turi[1]

Eötvös Loránd University, Department of Physical Chemistry, Budapest 112, P. O. Box 32, H-1518, Hungary

We have investigated the hydration dynamics in size selected water clusters with n=66, 104, 200, 500 and 1000 water molecules using molecular dynamics simulations. To study the most fundamental aspects of relaxation phenomena in clusters, we choose one of the simplest, still realistic, quantum mechanically treated test solute, an excess electron. The project focuses on the time evolution of the clusters following two processes, electron attachment to neutral equilibrated water clusters and electron detachment from an equilibrated water cluster anion. The relaxation dynamics is significantly different in the two processes, most notably restoring the equilibrium final state is less effective after electron attachment. Nevertheless, in both scenarios only minor cluster size dependence is observed. Significantly different relaxation patterns characterize electron detachment for interior and surface state clusters, interior state clusters relaxing significantly faster. This observation may indicate a potential way to distinguish surface state and interior state water cluster anion isomers experimentally. A

[1] E-mail: turi@chem.elte.hu, fax: (36)-1-372-2592.

comparison of equilibrium and non-equilibrium trajectories suggests that linear response theory breaks down for electron attachment at 200 K, but the results converge to reasonable agreement at higher temperatures. Relaxation following electron detachment clearly belongs to the linear regime.

Cluster relaxation was also investigated using two different computational models, one preferring cavity type interior states for the excess electron in bulk water, while the other simulating non-cavity structure. While the cavity model predicts appearance of several different hydrated electron isomers in agreement with experiment, the non-cavity model locates only cluster anions with interior excess electron distribution. The present simulations show that surface isomers computed with the cavity predicting potential show similar dynamical behavior to the interior clusters of the non-cavity type model. Relaxation associated with cavity collapse presents, however, unique dynamical signatures.

I. Introduction

Molecular processes that take place in aqueous environment are key to understanding the molecular level functions in living organisms. The direct transformation - breaking and formation - of chemical bonds is coupled to and significantly influenced by a more general background of molecular level relaxation events, hydration. The importance of hydration has been deeply appreciated and its mechanistic details are fairly well understood.[1,2] More work is needed, however, to reach detailed understanding of the couplings of the solvent motions to the energy levels of the solute particles. Significant recent efforts, both experimental and theoretical, have been invested in this direction.[3,4,5,6]

Studying hydration in aqueous systems with finite extensions (clusters, surfaces, interfaces) provides additional valuable insight into the relaxation phenomenon, since these systems can mimic anisotropic boundary conditions that are of high relevance in biochemical systems.[7,8] In addition, the more limited number of nuclear degrees of freedom available in these systems, in clusters in particular, may help to disentangle and identify the physically relevant nuclear modes of the relaxation. Influence of the molecules experiencing anisotropic environment on the relaxation may also be analyzed, although this aspect clearly increases the complexity of the issue. It is also of fundamental interest that the physical properties in increasing size clusters are expected to extrapolate to those of the bulk, an issue that can be readily tested and compared with experiment.

Here we examine hydration dynamics in various size water clusters using molecular dynamics simulation techniques. Molecular dynamics provides a direct tool for examining the microscopic details of the temporal behavior of molecular systems. Classical molecular dynamics has been applied extensively for clusters in the last decades.[9,10,11,12,13,14,15] Classical simulations, however, are unable to provide information even on the most basic quantum

aspects of hydration. Although simulations on clusters treating all electrons (or all valence electrons) quantum mechanically are quickly progressing to become routine procedures, ab initio molecular dynamics (AIMD) techniques are still somewhat limited in terms of system size and sampling efficiency. Mixed quantum-classical molecular dynamics (QCMD) simulations modeling solvent particles classically, while describing solutes quantum mechanically still offer a reasonable compromise between sophistication and effectiveness.[16,17,18] Negatively charged water clusters, also known as hydrated electron clusters,[19,20] can be viewed as one of the simplest conceivable solvent-solute systems, an ideal target for QCMD simulations. Within the QCMD framework, the quantum mechanical solute, the excess electron, having only electronic, but no nuclear degrees of freedom, is embedded in a classical bath of a handful of water molecules.[21,22,23] Despite the relative simplicity, water cluster anions still pose a challenging case for sophisticated theoretical[24,25,26] and experimental approaches.[27,28,29,30,31,32,33,34]

Although molecular dynamics simulations have provided a rather consistent picture of the hydrated electron system, as have been reviewed recently,[35] a few unanswered, nonetheless disturbing questions remain open. A notable problem concerns the structure of the hydrated electron. The more or less consensus, localized cavity structure[36,37,38] has been challenged by an alternative model,[39] a non-cavity type ("inverse-plum"[40]) electron distribution for the bulk hydrated electron. As another structural issue, there is still no agreement on where the excess electron is localized relative to the nuclear frame in water clusters, i.e. in interior or surface excess electronic states.[21,22,23,32,41,42,43,44,45] Since it is plausible that the main character of the relaxation is different in different localization modes, simulations of electron localization and/or electronic excitation in water cluster anions may provide clues on how to distinguish these isomers experimentally.

Recently AIMD simulations have been performed on water cluster anions using electronic density functional theory. [26,46,47,48] Extensive non-equilibrium simulations at this level, however, are non-existent. The main difficulty is that reliable sampling of non-equilibrium dynamics requires many parallel trajectories that may be beyond reasonable computational efforts using the AIMD technique. One-electron mixed quantum-classical simulations have been proved to be valuable in investigating and interpreting hydrated electron properties. [18,38,49,50,51,52,53] In the present paper, we apply QCMD simulations for the relaxation dynamics of water clusters. Two main non-equilibrium scenarios will be modeled and investigated in detail. In the first scheme, we add an excess electron to size-selected, neutral equilibrated clusters and follow the subsequent dynamics that eventually leads to equilibrium hydrated electron clusters. This process can be considered as a simplified model of the formation of water cluster anions by the collision of water clusters and slow electrons (Figure 1). We note that we are aware of one QCMD study by Barnett et al. that examined adiabatic solvation dynamics of an excess electron in water and ammonia clusters.[54] This early pioneering study, however, is limited both in terms of timescale, cluster size and sampling for our present purposes. In the second model, we investigate the reverse process and remove the excess electron from equilibrium hydrated electron clusters (Figure 2). The relaxation of the neutral cluster after removing the electron will be monitored back to its neutral equilibrium state. This scenario may be viewed as an approximation of the photodetachment experiments on hydrated electron clusters. In both processes, structural and energetic patterns of the relaxation will be examined and characterized. We also analyze the validity of linear response theory (LRT).[55] LRT predicts equivalence of the non-equilibrium relaxation functions to the corresponding equilibrium autocorrelation functions.[9] In order to obtain information on how the temperature affects cluster relaxation, we perform the simulations at two different sets of cluster internal energy, i. e. effective temperature. We

mention here that these two relaxation routes were originally applied in our previous work for electron solvation in bulk methanol.[56] Here, their application for water clusters opens novel interpretation possibilities.

Several one-electron pseudopotential models have been suggested to model the electron-water molecule interaction in mixed QCMD simulations.[18,39,53,57,58,59,60,61] The Turi-Borgis (TB) model[53] used in the present study has provided a consistent microscopic picture and a semi-quantitative agreement with experiment.[22,43,53,62,63,64]. This is the main motivation for using the TB potential in the present study. Two other models have been proposed more recently, the one by the Herbert group,[61] the other by Schwartz and his co-workers.[39] The Jacobson-Herbert (JH) model employs a polarizable water potential and rigid water molecules providing good agreement with experiment and moderately high-level ab initio calculations.[61] The TB and the JH potentials predict cavity model for the bulk hydrated electron.[53,61] The Larsen-Glover-Schwartz (LGS) potential[39] is based on a one-electron frozen-core pseudopotential theory[59,65] similar to the TB model.[66] Due to its different parametrization the LGS potential leads to a conceptually different non-cavity structure for the bulk hydrated electron.[39] Although the LGS potential have been criticized,[67,68] thoroughly analyzed, and compared to other cavity predicting models,[69] the problems with the model have not been addressed yet. More recent simulations have been published with the LGS potential that predict results compatible with certain sets of experimental observations.[40,70] This situation makes it necessary to further investigate the problem and test the models. Since both the TB and the LGS models employ the same water-water classical potential (simple point charge (SPC) model with flexibility),[71] it is reasonable to compare these two models directly and identify possible dynamical signatures associated with the different electron-water molecule potentials. For this reason, although the main part of the relaxation simulations will be executed within a computational model (TB potential) that prefers cavity structure for the

excess electron in water, for comparison, we also simulate water cluster anions with a non-cavity type LGS pseudopotential. Here only the dynamics of the hydrated electron clusters will be evaluated and compared using the two different models. Further comparison of the two pseudopotentials will be published elsewhere.

The structure of the remainder of the paper will be as follows. In Sec II, we summarize the basic features of the QCMD simulation techniques used in the present study. In Sec. III, we first analyze the non-equilibrium dynamics following electron attachment to neutral equilibrium clusters, then the removal of an excess electron from equilibrium anionic clusters, both using the TB potential. This is followed by a comparison of the simulations based on two different water molecule-electron pseudopotential models (TB and LGS potentials). Sec III also includes a comparison of the equilibrium and non-equilibrium response functions to test linear response. Sec IV provides a discussion and concludes the paper.

II. Methods

The simulations have been performed using a mixed quantum classical molecular dynamics method.[17] This method has been developed and employed intensely in the Rossky group (see references in Ref 35). We also used this method previously in a series of studies,[22,43,53,62,63,64] so here we focus only on its main features. Water molecules are described classically with a flexible three-site potential,[71] while the excess electron is represented by its wave function on a finite grid, evenly distributed in a cubic box. We use two different size grids depending on the investigated relaxation scenario (see below). The smaller one, with box side of 18.17 Å, has 16x16x16 grid points (Basis 1), while the larger one, with box side of 36.34 Å has 32x32x32 grid points. The electron-water molecule interaction is modeled by a pseudopotential that predicts cavity-type hydrated electron structure in bulk simulations.[53] The time-independent Schrödinger equation for the excess electron is solved in the potential

field of the classical water molecules using an iterative and block Lanczos procedure.[17] During the time evolution of the system the water molecules move under the combined influence of the electron and the other molecules. The quantum force is evaluated applying the Hellman-Feynman theorem. The dynamics is adiabatic, that is the classical molecules move on the ground state excess electronic potential surface. The Verlet algorithm is used to integrate the equations of motion with a time step of 1 fs.[72] The simulated water clusters contain n = 66, 104, 200, 500 and 1000 water molecules. The simulations were carried out in the microcanonical ensemble.

We perform two types of computer experiments, electron removal from water cluster anions and electron addition to neutral water clusters. The non-equilibrium trajectories are initiated from long equilibrium "reference" trajectories. Electron removal trajectories are launched from configurations along equilibrium water cluster anion trajectories, while electron addition from equilibrium neutral clusters. The reference trajectories are equilibrated at 200 K, consistent with previous simulations. To evaluate the effect of temperature, the simulations have also been performed at 250 K. The length of the equilibrium trajectories are 200 ps and 300 ps for the anionic and the neutral clusters, respectively. Since the electron is well localized along the equilibrium cluster anion trajectory, here it suffices to use the smaller Basis I. The reference trajectories of the neutral water clusters are monitored by computing the electron's binding energy to these clusters. Since these binding energies are small, the electron becomes more delocalized, and this requires the application of a more diffuse, larger basis, Basis II. The initial configurations for the non-equilibrium relaxation trajectories are selected from the last 100 ps portion of the equilibrium trajectories separated equidistantly by 1 ps segments. Overall 100 such non-equilibrium trajectories are run and analyzed for each cluster size and temperature.

The simulations with the LGS electron-water molecule pseudopotential follow the same protocol, except for the fact that due to its more rugged potential surface, the evaluation of the LGS potential requires denser spatial grid. For this a grid of 18.17 Å length with 32x32x32 grid points proved to be sufficient. The LGS results are based on 50 ps long equilibrium trajectories at T = 200 K effective temperature. The non-equilibrium relaxation trajectories are launched from configurations separated equidistantly by 0.5 ps segments.

III. Results

Electron attachment. Water cluster anions are usually prepared in molecular jets after an expansion of water vapor.[19,20,73] The initially formed neutral water clusters collide with slow secondary electrons of an electron source, and bind the electrons. Although the exact mechanism of cluster formation and the following electron attachment is not known, simple models of the process can be invented and studied by molecular dynamics.[54,56,62] In the simplest possible scenario we add an electron to equilibrated neutral clusters, a process modeling "collision" with a zero kinetic energy electron. Technically, we turn on the excess electron - water cluster interaction instantaneously during a classical MD trajectory. We analyzed the electron localization sites on equilibrium neutral clusters previously, and found that clusters bind the electron very weakly, exclusively on the surface of the cluster.[62] In this section we investigate the dynamics of these initially weakly bound species relaxing to stable hydrated electron clusters. Figure 1 illustrates the electron attachment process starting from a neutral water cluster (n=500). The lowest unoccupied molecular orbital (LUMO) of the cluster is shown with a mesh isosurface in the left side of the figure. Electron attachment takes place instantaneously in the model, the electron occupying the highest occupied molecular orbital (HOMO) of the anion illustrated with a solid electron density isosurface in the middle part of the figure. After 1 ps molecular and electronic relaxation leads to a (partially) relaxed

water cluster anion structure (right side of the figure). The isosurfaces show 80 % probability of finding the excess electron.

Figure 3 shows the non-equilibrium response functions ($S(t)$, Eq (1)) of electron hydration[51] for the electron's ground state energy, equivalent to the negative of the vertical detachment energy of the excess electron from the cluster (VDE) in the present non-polarizable model.

$$S(t) = \frac{\overline{E}(t) - \overline{E}(\infty)}{\overline{E}(0) - \overline{E}(\infty)} \tag{1}$$

In Eq. (1), the overbar indicates non-equilibrium averages, $\overline{E}(0)$ corresponds to the initial eigenvalue of the weakly bound excess electron, while $\overline{E}(\infty)$ is the ground state electronic energy of the equilibrium cluster anions. The computed ground state energies for different size surface state clusters correspond well to our previous simulations increasing in strength from -1.1 eV (n = 66) to -3.1 eV (n = 1000) at 200 K,[22,43] and these results are independent of temperature. We note that initially the electron localizes on the surface of the cluster, and it remains there during the 1 ps length of the non-equilibrium runs. We have also performed extended equilibrium simulations of the cluster anions that indicate that surface stabilized cluster anions persist on the several hundred ps timeframe of the simulation at 200 K. Increasing the temperature does not influence the localization mode of the electron, except for the largest examined cluster size (n = 1000) where the electron diffuses into the interior after ~30 ps at 250 K. The same n = 1000 cluster anion at 200 K does not undergo such transition during the length of the equilibrium trajectory. This observation obviously does not mean that there are no other persisting interior state cluster anions at these temperatures.[22,43] We return to this issue in the next section.

The normalized non-equilibrium response functions show distinct similarity, although relaxation becomes slightly more efficient with increasing size (Figure 3). Nevertheless, the

relaxation is surprisingly slow, after 1 ps only ~40 % of the relaxation is completed at 200 K. The temperature increase to 250 K causes faster hydration with ~60 % of the full relaxation after 1 ps. The initial ultrafast Gaussian part (~10 fs timescale) of the relaxation, usually attributed to inertial rotational motion,[74] contributes less than 10 % to the relaxation. We found previously that initially the electron localizes on dangling hydrogen atoms on the surface.[62] It is now reasonable to suggest that initially the rotation of the free surface OH hydrogen atoms accommodate the excess electron.

We also analyzed the correlation of the geometric changes of the electron distribution and the dipole moment of the clusters during the localization and the subsequent stabilization that follows electron attachment. The two processes proceed sequentially and clearly distinguishable, as illustrated in Figure 4 for the n = 500 surface state stabilized cluster. The radius of the electron collapses from its initial, diffuse 11 Å to about 6 Å within the first ~20 fs, matching the ultrafast part of the energy relaxation. At the same time the dipole moment of the molecular frame jumps from 19 D to 28 D indicating local rearrangement (rotation) of a few molecules in contact with the electron. This is a localization step. A significantly slower process follows after 20 fs. The electron shrinks further from ~ 6 Å to ~ 4 Å by the end of the non-equilibrium trajectories producing ~20 % of the energy relaxation, while the dipole moment increases another 10 D. The remaining ~ 60-70 % portion of the relaxation that takes place after the 1 ps time window of the trajectories is associated with only a relatively smaller contraction of the electron from 4 Å to the equilibrium 2.5-2.6 Å. At the same time, the complex cooperative rearrangement of the hydrogen-bonded network slowly continues leading to further significant increase (more than 20 D) of the dipole moment up to ~ 60 D.

For comparison with the non-equilibrium relaxation functions we computed the normalized equilibrium time correlation function of the ground state energy of the reference trajectory, that of the equilibrium hydrated electron cluster.

$$C(t) = \frac{\langle \delta E(0) \delta E(t) \rangle}{\langle \delta E^2 \rangle} \quad (2)$$

In Eq. (2) the brackets indicate equilibrium averages, and δ symbolizes deviations from equilibrium values (fluctuation). According to the linear response (LR) theory the normalized non-equilibrium relaxation function *S(t)* of the solvation energy is equal to the (equilibrium) time correlation function of the fluctuations of the potential difference monitored by the solute.[9,55] Qualitatively, LR theory states that the solvent relaxes after an instantaneous, small perturbation in the same manner as it does after an equilibrium fluctuation. The quantitative mathematical relationship is based on first-order perturbation theory, and shows the equivalence of *S(t)* and *C(t)* functions.[55] LRT has been analyzed and tested for the hydration of classical ions[5,9] and the hydrated electron,[51,75] as well, in clusters only for classical ions.[9] These studies, however, reached contradictory conclusions whether LRT holds[9,51] or not.[5,75] We note that the investigated two scenarios for the electron hydration in clusters in the present work are related to studies on the solvent response on step changes in classical solute charges (charge creation and annihilation).[9] Figure 5 shows both the equilibrium and the non-equilibrium correlation functions of Eqs 1 and 2 for two cluster sizes at 200 K and 250 K. The results clearly show that LRT does have limited validity in cold clusters for electron attachment but as the temperature increases the deviation between the relaxation functions tends to disappear. This suggests a tendency that LRT may have more justified applicability at higher temperatures. We note that this observation pertains to cluster anions that bind the excess electron in surface states. Since electron attachment always takes place via surface states (in the TB model),[62] we have no direct way to examine electron attachment to interior states in clusters. In the next section we demonstrate that for the reverse process, electron detachment, the dynamics of both localization modes can be readily observed and characterized.

Electron detachment. In electron detachment experiments high-energy photons hit water cluster anions and remove the excess electron from the cluster.[27,28,31,32,34] The kinetic energy of the detached electron (photoelectron) is then measured, and its binding energy to the cluster is determined. Our second computer experiment models the relaxation of neutral water clusters after removing the excess electron from anionic water clusters. In practice, this means turning off the electron-water cluster interaction in water cluster anions instantaneously, and following the dynamics of the remaining neutral cluster. Once the electron is removed, the neutral cluster relaxes, and this process is monitored by the binding energy of an excess electron, as if the electron were still bound to the neutral cluster. In other words, we compute the binding energy of a fictive excess electron to the nuclear configurations of the neutral cluster along the trajectory of the relaxing neutral cluster. Figure 2 illustrates the electron detachment process starting from an equilibrium water cluster anion. The HOMO of the cluster anion is shown with a solid isosurface on the left side of Figure 2. Electron detachment takes place instantaneously in the model, leaving a neutral cluster in the geometry of the equilibrated anion with a LUMO that is shown with a mesh electron density isosurface in the middle of the figure. After 1 ps, molecular relaxation results in a (partially) relaxed neutral water cluster structure (right side, Figure 2) that would be a non-relaxed configuration for an excess electron (see the diffuse LUMO on right side of the figure). The isosurfaces show 80 % probability of finding the excess electron.

At the outset of the analysis we note that the present TB model locates at least two possible isomers of hydrated electron clusters for sizes larger than ~200.[43] Therefore modeling electron detachment is necessarily more complex than the electron attachment scenario, where only surface state relaxation takes place. For surface states, we initiate the dynamics from the same equilibrium anionic trajectories that were listed in the previous

section, while the two investigated interior state clusters (n = 500 and 1000) begin the relaxation from trajectories with binding energies of -3.2 eV and -3.7 eV, respectively. These numbers are consistent with previous simulations,[22,43] and also agree reasonably with experiments.[32] The relaxation of the two types of isomers exhibits markedly different patterns as shown in Figure 6. Figure 6 contains the normalized non-equilibrium relaxation function for both surface state and interior state cluster anions at 200 K. Both types of isomers show strikingly uniform behavior within the group indicating no or minor size effect. For surface state clusters, one observes an ultrafast solvation component with a gaussian characteristic time of ~10 fs that contributes ~50 % to the relaxation. Fluctuations on two separate timescales are apparent at the early times of the relaxation (appearing at ~20 fs) with ~20 fs and ~40 fs characteristic times corresponding well to HOH bending vibrations and hindered rotations, correspondingly. These modes of surface water molecules restore the hydrogen-bonding network of the neutral surface most effectively after the electron is removed from the surface. Fourier transform of the time evolution of the ground state energy of the electron, fictively bound to the neutral cluster, maps the neutral cluster's dynamics (not shown). It reveals that both translation, libration and HOH bending vibrations contribute to modulating energy level fluctuations.

Interior state clusters show a more dramatic relaxation pattern. The ultrafast regime (~5 fs characteristic time) is responsible for ~70 % of the total relaxation, and the following recurrences show only ~40 fs timescale fluctuations. The frequency of this fluctuation matches the rate of variation of the radius of the excess electron as illustrated in Figure 7. This clearly suggests a mechanistic picture of the relaxation. Once the electron is removed from inside the cluster, the hydrogen atoms that initially point to the electron find themselves repelled by other hydrogen atoms across the cavity. To avoid this repulsion the hydrogen

atoms rotate away creating a less accommodating environment for the "test" electron with a smaller stabilization energy. The oxygen non-bonding electron pair on the rotating water starts driving the excess electron out of the cavity. During this process the electron takes up a more diffuse spatial distribution. Meanwhile the cavity shrinks in size as indicated by the gradual increase of the baseline of the radius curve. We note that it takes ~400 fs for the cavity to completely disappear as indicated by the asymptotic plateau of the electron's radius at about 9 Å (not shown). By this time the electron's binding site diffuses out to the surface of the cluster.

The reference trajectory of the electron detachment equilibrium response function is that of a neutral cluster. The $C(t)$ function is computed from the binding energies of an electron to the neutral cluster along the trajectory, with the electron not influencing the time evolution of the neutral cluster itself. Since the electron localizes on the surface of the neutral clusters in all examined cases, LRT can be assessed only for surface state isomers. We observe that LRT holds very nicely for electron detachment for all examined cluster sizes, even at 200 K, as illustrated in Figure 8.

Comparison of hydrated electron models. In the next section we briefly compare hydrated electron cluster adiabatic dynamics simulated with two presently available pseudopotential models, that of Larsen, Glover and Schwartz (LGS),[39] and the one used in the present work, the TB model.[53] The first important observation is that, while the TB potential observes both interior and surface state clusters in simulations,[22,43] the electron always localizes and remains in the interior of the clusters in the LGS model. The most basic energetic and structural data (i.e. the ground state energy, the radius of gyration of the excess electron, and the steady-state absorption spectra of the electron) will be analyzed in a separate paper. We note here that these parameters predicted by the LGS model seem to be less

consistent with cluster anion measurements than those predicting cavity structure in bulk.[22,23,43]

Figure 9 shows non-equilibrium relaxation functions for both electron attachment and electron detachment scenarios computed with the LGS model. Interestingly, the LGS model shows qualitatively similar dynamics for all clusters where the TB model predicts surface states. The only clear difference appears in the dynamics of the collapse of the interior cavity structure, that has no counterpart in the LGS model. Relatively minor differences also appear in the similar cases, too. For example, LGS interior (non-cavity) state relaxation exhibits monotonic size dependence, larger clusters relaxing more slowly, while TB surface state dynamics are less uniform in the electron attachment case. These findings suggest that the dominant features of the relaxation dynamics are likely to be dictated by the common factor of the two potentials, the water-water potential. The different electron-water potential and the localization mode (surface or interior non-cavity) are responsible for the minor deviations. As another similarity, analysis of the corresponding equilibrium response functions of the ground state energy of the electron in the LGS model revealed similar breakdown in LR as with the TB potential (not shown) in the electron attachment case.

Figure 9 also illustrates the relaxation dynamics following electron detachment using the LGS model. Here, the relaxation patterns with the LGS model clearly parallel those computed for the surface state relaxation of the TB model. Once again, this similarity reflects the dynamical features of the water potential and the fact that both models lack interior cavity in the investigated clusters. The electron removal from the interior of larger cluster anions in the TB model leads to the collapse of the cavity, an event that is not present in either the TB surface relaxation or in the LGS interior relaxation schemes. The dynamic signature of cavity collapse appears to be characteristic and clearly distinguishes cavity structures from non-

cavity structures. This dissimilarity in dynamics may be sufficient for the experimental observation and differentiation between cavity vs. non-cavity type structures, and/or interior state (with cavity) vs. surface state structures in cluster anions.

IV. Discussion and Conclusions

We have performed a mixed quantum-classical molecular dynamics study on the adiabatic hydration of a ground state excess electron in various size water clusters. Two scenarios were modeled, electron attachment to equilibrium neutral clusters and electron detachment from equilibrium water cluster anions. The dynamics shows remarkable differences in the two processes. Relaxation of the water molecules following electron attachment is notably slower than relaxation after electron detachment. Electron attachment always starts in a surface electronic state with a diffuse excess electron distribution. Inertial rotation of surface water molecules with dangling hydrogen atoms dominate the relaxation at the shortest timescale. This is followed by a relatively slow (ps timescale) rearrangement of the hydrogen bonding network leading to increasing dipole moment of the molecular frame. Previous simulations of excess electron attachment to neutral water clusters at room temperature using a different one-electron model (for n=256 cluster),[54] and using an AIMD technique (for n=32 cluster)[48] predict timescales and molecular level events that are consistent with the present findings. The reverse process can start from two isomeric states, from surface state clusters and interior state clusters. The assignment of the experimentally available data[27,32,33,44,45] to these isomers still generates intense debates.[22,23,32,41,44,76,77] Therefore, it is important to anticipate and examine physical properties that are potentially different in these two states. Here we observe that the two types of cluster isomers relax with significant differences, interior state cavity type clusters relaxing more efficiently than surface cluster anions. This effect is the signature of the collapsing cavity, and we suggest that this effect

may be observed experimentally. We point out, however, that up to now, the experimental data and their assignments were based on the measurement of the properties of the photodetached electron (i.e. kinetic energy). It would require a conceptually different type of experiment (most likely a complicated task) to monitor neutral cluster dynamics following the removal of an electron from the cluster anion.

We observed minor cluster size effects on the relaxation dynamics, the non-equilibrium relaxation functions being very similar within the two scenarios. Linear response theory was also tested in the present study. We found that linear response breaks down for electron attachment at low temperatures, but as the temperature increases the match between equilibrium and non-equilibrium response functions significantly improves. The electron detachment case for surface state isomers clearly belongs to the linear regime at both investigated temperatures. We note that formally neutral water clusters can be viewed as water cluster anions excited all the way to electron detachment. In the most general sense of LRT, correlation functions on the ground state and the excited state surfaces should be identical,[78] a requirement that clearly does not hold for neutral water cluster and water cluster anion equilibrium correlation functions.

Comparison of cluster dynamics using two different pseudopotential models also provides valuable information. We found distinct dynamical patterns that may help evaluating the applicability of the two investigated pseudopotentials, one predicting cavity structure, the other a conceptually different, non-cavity type hydrated electron structure. A notable difference is that LGS model predicts electron attachment to neutral water clusters directly into the interior of the cluster, while TB model always simulates surface state attachment at the outset. In LGS, the electron relaxes by pulling water molecules under its electron cloud increasing water density locally. In the TB model the initial surface state electron relaxes

either at the surface or, at larger cluster sizes, diffuses into the interior of the clusters. During this penetration the electron occupies a cavity, pushing water molecules away from its vicinity. Cluster anion experiments suggest several different motifs of VDE with size.[32] While TB model simulated at least three (stable and metastable) groups of clusters,[22,43,64] the LGS model does not appear to reproduce this observation. We also note that the other recently developed cavity preferring JH model[61] also predicts several different VDE patterns with size,[23] and is consistent with experiments. Ab initio molecular dynamics simulations on cluster anions also support the existence of surface state water cluster anions.[79]

Since the LGS potential calculates only internally hydrated electrons with no-cavity, any dynamical signal that is associated with a collapse of a cavity would support the cavity types interior state (as seen in the TB model). This difference should also exist in bulk water. We mention here that other physical properties (i.e. structure, absorption spectrum, etc.) can also be tested for assessing the potential models but that analysis will be a topic of a different paper. Our previous short analysis suggests that consistency of the structural, energetic and spectroscopic data computed with the LGS potential in comparison with cluster experiments may be questionable.[67]

Acknowledgments

This work was supported by a research grant to LT from the National Research Fund of Hungary (OTKA, K104237).

Figure Captions

Figure 1. A schematic illustration of the relaxation of a n = 500 water cluster following excess electron attachment to the equilibrium neutral cluster. The mesh electron density isosurface shows the LUMO of the neutral cluster, while the solid surface indicates the HOMO of the cluster anion. The isosurfaces show 80 % probability of finding the excess electron.

Figure 2. A schematic illustration of the relaxation of a n = 500 water cluster following excess electron detachment from the equilibrium water cluster anion. The solid electron density isosurface shows the HOMO of the cluster anion, while the mesh surface indicates the LUMO of the neutral cluster. Top: relaxation of a surface state cluster anion, bottom: relaxation of an interior state cluster anion. The isosurfaces show 80 % probability of finding the excess electron.

Figure 3. Non-equilibrium response functions (eq. 1) for excess electron attachment to equilibrated neutral water clusters of different size. The simulated sizes are n = 66 (red), 104 (green), 200 (blue), 500 (cyan) and 1000 (magenta).

Figure 4. Geometric relaxation in n = 500 water clusters following electron attachment. The radius of gyration for the electron is shown by a solid red line, the dipole moment of the molecular frame by a dashed blue line.

Figure 5. Equilibrium (eq. 2) and non-equilibrium (eq. 1) response functions for electron attachment to neutral water clusters for two selected cluster sizes, n = 200 (red) and 500 (blue). Equilibrium functions: dashed lines, non-equilibrium functions: solid lines.

Figure 6. Normalized non-equilibrium relaxation functions for excess electron detachment from equilibrated anionic water clusters of different size at 200 K. The simulated sizes are n =

66 (red), 104 (green), 200 (blue), 500 (cyan) and 1000 (magenta). Figure shows functions for both surface state (solid lines) and interior state cluster anions (dashed lines).

Figure 7. Normalized non-equilibrium response function (left side scale, solid red line) and the radius of the excess electron (right side scale, dashed blue line) for the electron detachment from n = 1000 interior state water cluster anion at 200 K.

Figure 8. Normalized equilibrium (eq. 2) and non-equilibrium (eq. 1) response functions for electron detachment from anionic water clusters for two selected cluster sizes, n = 200 (red) and 500 (blue) at 200 K. Equilibrium correlation functions: dashed lines, non-equilibrium response functions: solid lines.

Figure 9. Normalized non-equilibrium relaxation functions for excess electron attachment to neutral water clusters (solid lines) and electron detachment from equilibrated anionic water clusters (dashed lines) at 200 K computed with the LGS model. The simulated cluster sizes are n = 66 (red), 104 (green), 200 (blue), 500 (cyan) and 1000 (magenta).

Figures:

Figure 1.

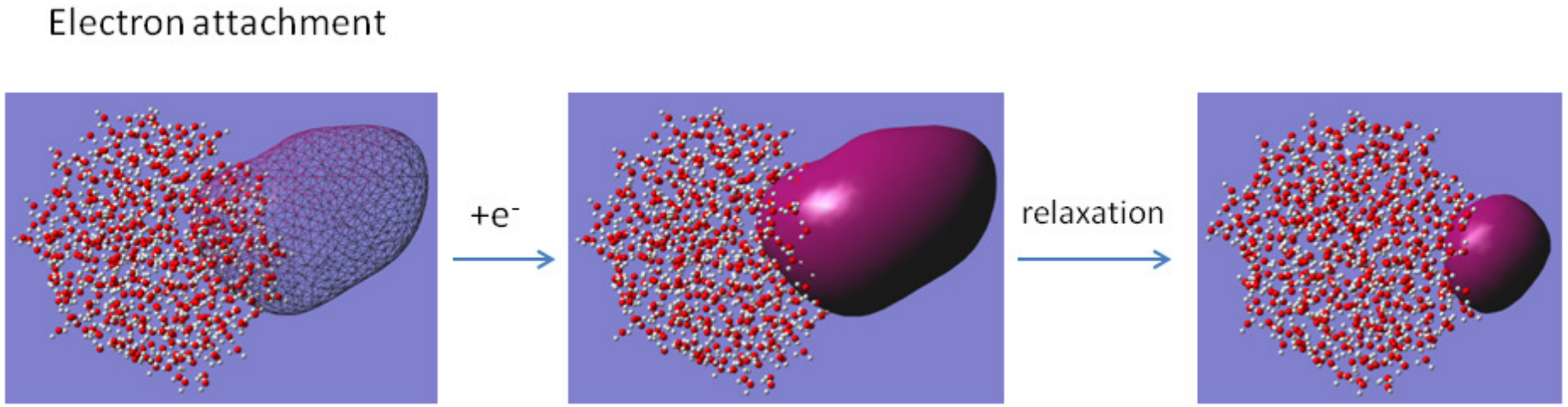

Figures:

Figure 2.

Electron detachment: surface states

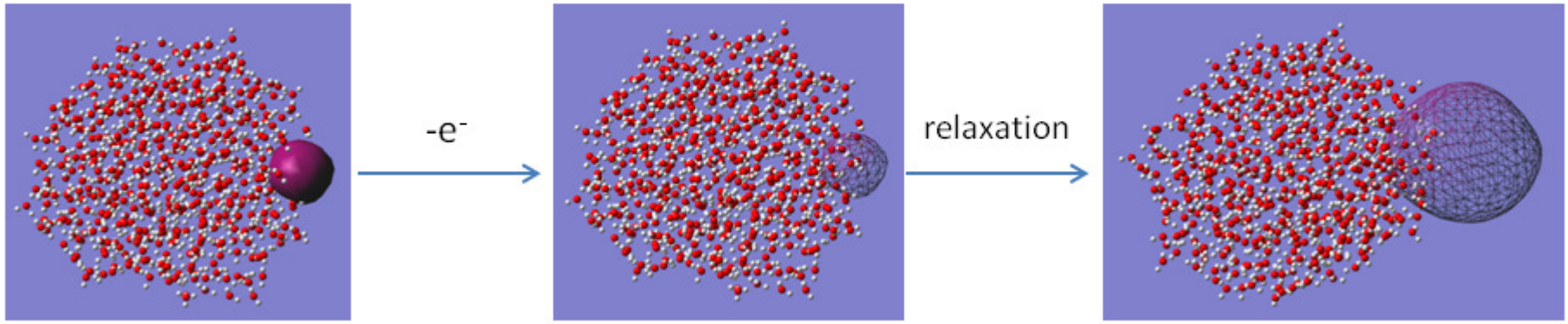

Electron detachment: interior states

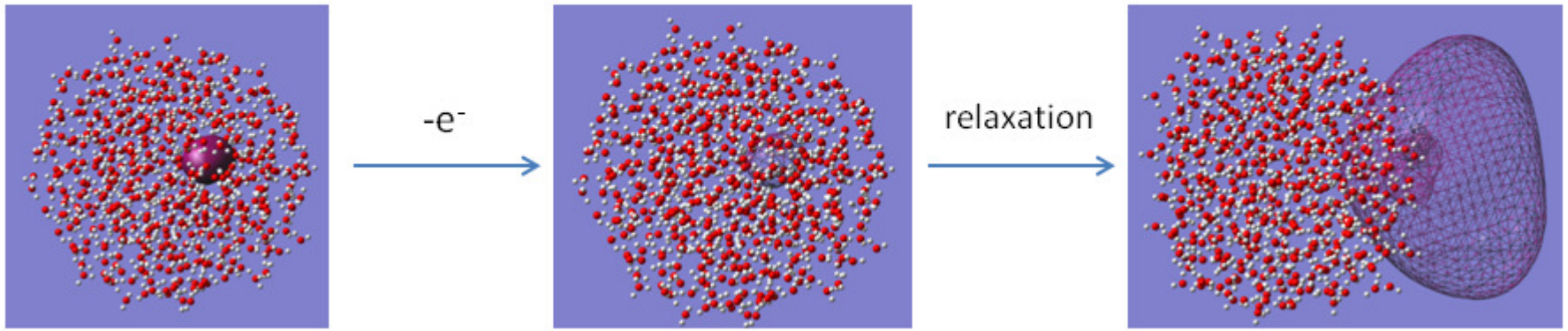

Figures:

Figure 3.

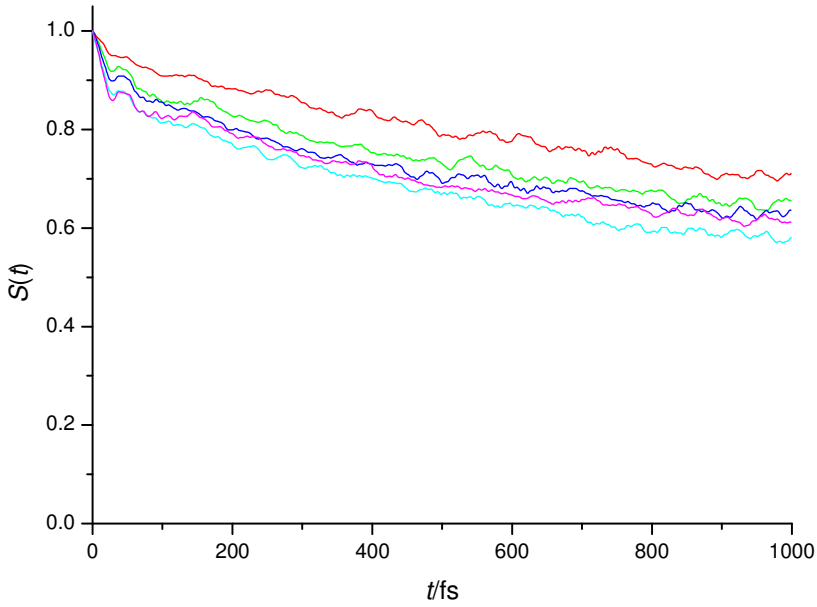

Figures:

Figure 4.

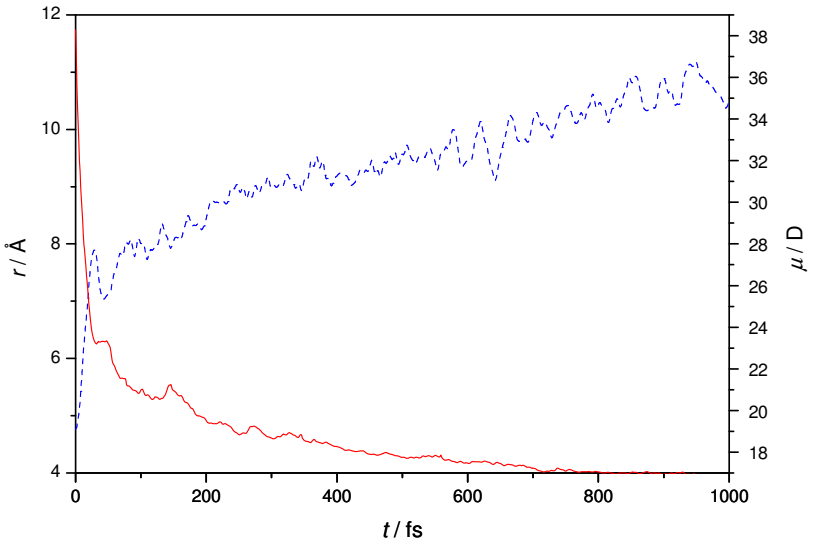

Figures:

Figure 5.

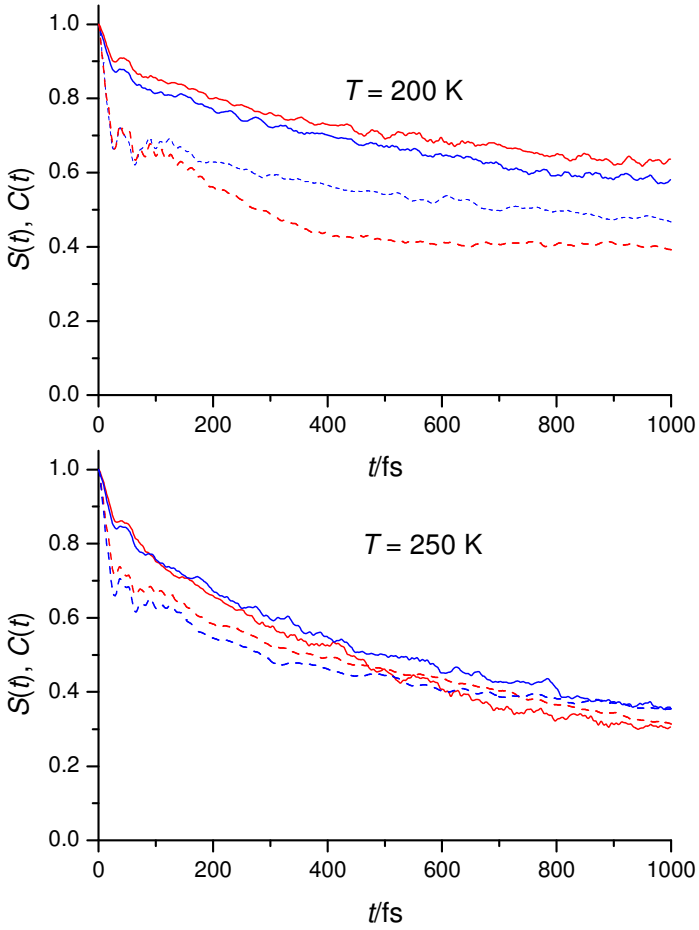

Figures:

Figure 6.

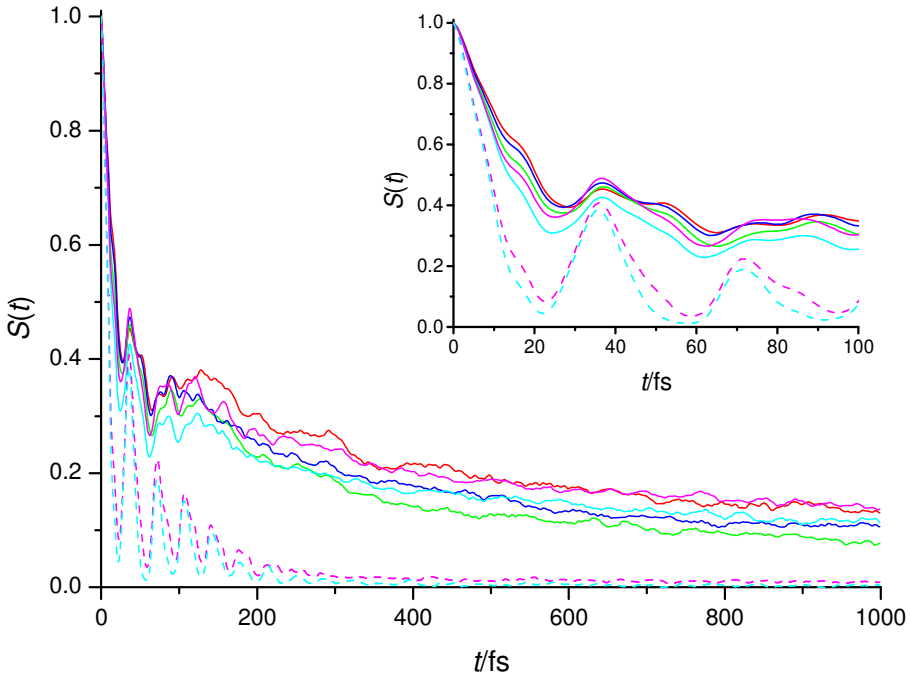

Figures:

Figure 7.

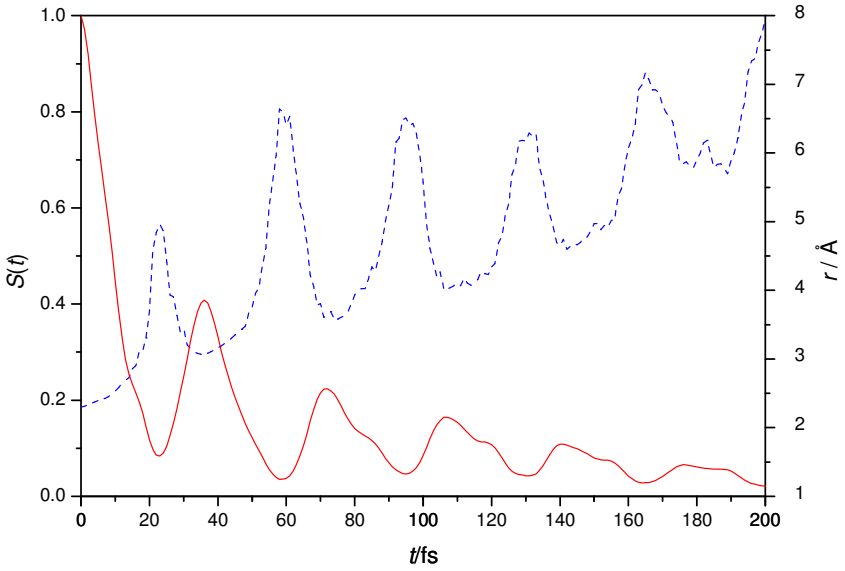

Figures:

Figure 8.

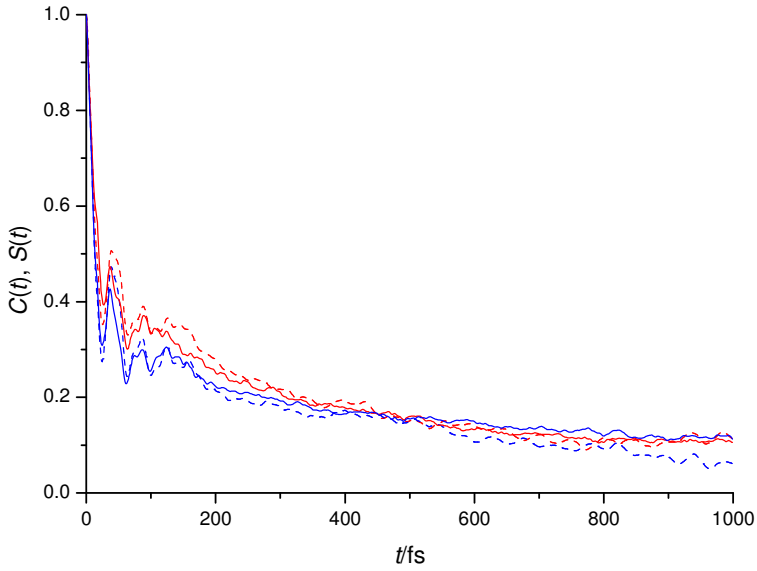

Figures:

Figure 9.

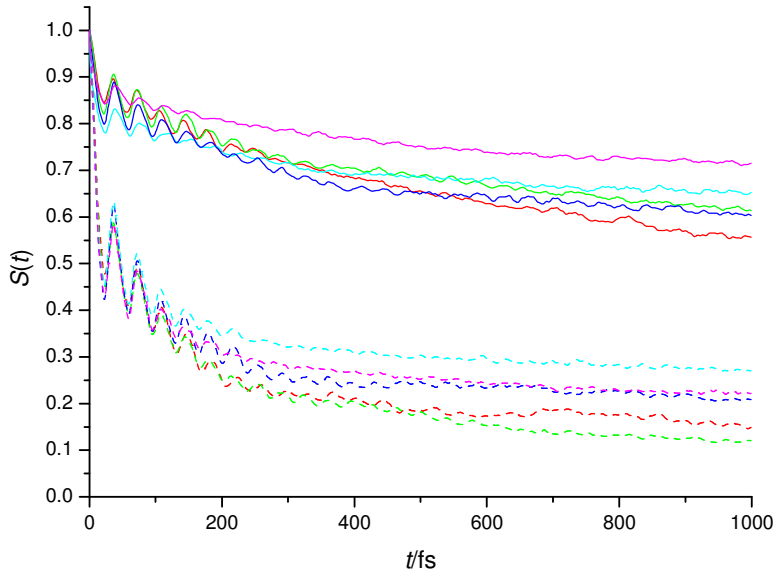

References

[1] H. Ohtaki and T. Radnai, Chem. Rev. **93**, 1157 (1993).

[2] B. Bagchi and B. Jana, Chem. Soc. Rev. **39**, 1936 (2010).

[3] R. H. Coridan, N. W. Schmidt, G. H. Lai, R. Godawat, M. Krisch, S. Garde, P. Abbamonte, and G. C. L. Wong, Phys. Rev. Lett. **103**, 237402 (2009).

[4] F. Messina, O. Bräm, A. Cannizzo and M. Chergui, Nat. Commun. **4**, 2119 (2013).

[5] P. E. Videla, P. J. Rossky, and D. Laria, J. Chem. Phys. **139**, 164506 (2013).

[6] S. Bogatko, E. Cauet, P. Geerlings, and F. De Proft, Phys. Chem. Chem. Phys. **16**, 3807 (2014).

[7] B. Bagchi, Chem. Rev. **108**, 3197 (2005).

[8] A. C. Fogarty, E. Duboué-Dijon, F. Sterpone, J. T. Hynes, and D. Laage, Chem. Soc. Rev. **42**, 5672 (2013).

[9] M. Maroncelli, and G. R. Fleming, J. Chem. Phys. **89**, 5044 (1988).

[10] L. S. Sremeniak, L. Perera, and M. I. Berkowitz, Chem. Phys. Lett. **218**, 377 (1994).

[11] L. S. Sremeniak, L. Perera, and M. I. Berkowitz, J. Phys. Chem. **100**, 1350 (1996).

[12] I.-C. Yeh, L. Perera, and M. I. Berkowitz, Chem. Phys. Lett. **264**, 31 (1997).

[13] P. Jungwirth, and D. J. Tobias, J. Phys. Chem. B **105**, 10468 (2001).

[14] P. Jungwirth, and D. J. Tobias, J. Phys. Chem. B **106**, 6361 (2002).

[15] P. Jungwirth, and D. J. Tobias, Chem. Rev. **106**, 1259 (2006).

[16] Z. Kotler, E. Neria and A. Nitzan, Comput. Phys. Commun. **63**, 243 (1991).

[17] F. A. Webster, P. J. Rossky and R. A. Friesner, Comput. Phys. Commun. **63**, 494 (1991).

[18] A. Staib and D. Borgis, J. Chem. Phys. **103**, 2642 (1995).

[19] M. Armbruster, H. Haberland, and H. G. Schindler, Phys. Rev. Lett. **47**, 323 (1981).

[20] H. Haberland, H. G. Schindler and D. R. Worsnop, Ber. Bunsenges. Phys. Chem. **88**, 270 (1984).

[21] R. N. Barnett, U. Landman, C. L. Cleveland, and J. Jortner, Phys. Rev. Lett. **59**, 811 (1987).

[22] L. Turi, W.-S. Sheu, and P. J. Rossky, Science **309**, 914 (2005).

[23] L. D. Jacobson, and J. M. Herbert, J. Am. Chem. Soc. **133**, 19889 (2011).

[24] T. Sommerfeld, A. DeFusco, and K. D. Jordan, J. Phys. Chem. A **112**, 11021 (2008).

[25] J. M. Herbert, and M. Head-Gordon, Phys. Chem. Chem. Phys. **8**, 68 (2006).

[26] O. Marsalek, F. Uhlig, J. VandeVondele, and P. Jungwirth, Acc. Chem. Res. **45**, 23 (2012).

[27] J. V. Coe, G. H. Lee, J. G. Eaton, S. T. Arnold, H. W. Sarkas, K. H. Bowen, C. Ludewigt, H. Haberland, and D. R. Worsnop, J. Chem. Phys. **92**, 3980 (1990).

[28] P. Ayotte, and M. A. Johnson, J. Chem. Phys. **10**6, 811 (1997).

[29] A. E. Bragg, J. R. R. Verlet, A. Kammrath, O. Cheshnovsky, and D. M. Neumark, Science **306**, 669 (2004).

[30] D. H. Paik, I-R. Lee, D.-S. Yang, J. S. Baskin, and A. H. Zewail, Science **306**, 672 (2004).

[31] N. I. Hammer, J.-W. Shin, J. M. Headrick, E. G. Diken, J. R. Roscioli, G. H. Weddle, and M. A. Johnson, Science **306**, 675 (2004).

[32] J. R. R. Verlet, A. E. Bragg, A. Kammrath, O. Cheshnovsky, and D. M. Neumark, Science **307**, 93 (2005).

[33] F. Zappa, S. Denifl, I. Mähr, A. Bacher, O. Echt, T. D. Märk, and P. Scheier, J. Am. Chem. Soc. **130**, 5573 (2008).

[34] O. T. Ehrler, and D. M. Neumark, Acc. Chem. Res. **42**, 769 (2009).

[35] L. Turi, and P. J. Rossky, Chem. Rev. **112**, 5641 (2012).

[36] R. A. Ogg, J. Am. Chem. Soc. **68**, 155 (1946).

[37] L. Kevan, Radiat. Phys. Chem. **17**, 413 (1981).

[38] J. Schnitker, and P. J. Rossky, J. Chem. Phys. **86**, 3471 (1987).

[39] R. E. Larsen, W. J. Glover, and B. J. Schwartz, Science **329**, 65 (2010).

[40] J. R. Casey, A. Kahros, and B. J. Schwartz, J. Phys. Chem. B **117**, 14173 (2013).

[41] D. M. Bartels, J. Chem. Phys. **115**, 4404 (2001).

[42] R. N. Barnett, U. Landman, C. L. Cleveland, and J. Jortner, J. Chem. Phys. **88**, 4429 (1988).

[43] Á. Madarász, P. J. Rossky, and L. Turi, J. Chem. Phys. **130**, 124319 (2009).

[44] J. V. Coe, S. M. Williams, and K. H. Bowen, Int. Rev. Phys. Chem. **27**, 27 (2008).

[45] G. B. Griffin, R. M. Young, O. T. Ehrler, and D. M. Neumark, J. Chem. Phys. **131**, 194302 (2009).

[46] T. Frigato, J. VandeVondele, B. Schmidt, C. Schütte, and P. Jungwirth, J. Phys. Chem. A **112**, 6125 (2008).

[47] O. Marsalek, F. Uhlig, and P. Jungwirth, J. Phys. Chem. C **114**, 20489 (2010).

[48] O. Marsalek, F. Uhlig, T. Frigato, B. Schmidt, and P. Jungwirth, Phys. Rev. Lett. **105**, 043002 (2010).

[49] J. Schnitker, K. Motakabbir, P. J. Rossky, and R. Friesner, Phys. Rev. Lett. **60**, 456 (1988).

[50] P. J. Rossky, and J. Schnitker, J. Phys. Chem. **92**, 4277 (1988).

[51] B. J. Schwartz, and P. J. Rossky, J. Chem. Phys. **101**, 6902 (1994).

[52] B. J. Schwartz, and P. J. Rossky, Phys. Rev. Lett. **72**, 3282 (1994).

[53] L. Turi, and D. Borgis, J. Chem. Phys. **117**, 6186 (2002).

[54] R. N. Barnett, U. Landman, and A. Nitzan, J. Chem. Phys. **91**, 5567 (1989).

[55] W. Bernard, and H. B. Callen, Rev. Mod. Phys. **31**, 1017 (1959).

[56] L. Turi, P. Mináry, and P. J. Rossky, Chem. Phys. Lett. **316**, 465 (2000).

[57] C. D. Jonah, C. Romero, and A. Rahman, Chem. Phys. Lett. **123**, 209 (1986).

[58] A. Wallqvist, D. Thirumalai, and B. J. Berne, J. Chem. Phys. **86**, 6404 (1987).

[59] J. Schnitker, and P. J. Rossky, J. Chem. Phys. **86**, 3462 (1987).

[60] R. N. Barnett, U. Landman, C. L. Cleveland, and J. Jortner, J. Chem. Phys. **88**, 4421 (1988).

[61] L. D. Jacobson, and J. M. Herbert, J. Chem. Phys. **133**, 154506 (2010).

[62] L. Turi, Á. Madarász, and P. J. Rossky, J. Chem. Phys. **125**, 014308 (2006).

[63] Á. Madarász, P. J. Rossky, and L. Turi, J. Chem. Phys. **126**, 234707 (2007).

[64] Á. Madarász, P. J. Rossky, and L. Turi, J. Phys. Chem. A **114**, 2331 (2010).

[65] J. C. Phillips, and L. Kleinman, Phys. Rev. **116**, 287 (1959).

[66] L. Turi, M.-P. Gaigeot, N. Levy, and D. Borgis, J. Chem. Phys. **114**, 7805 (2001).

[67] L. Turi, and Á. Madarász, Science, **331**, 1387-c (2011).

[68] L. D. Jacobson, and J. M. Herbert, Science, **331**, 1387-d (2011).

[69] J. M. Herbert, and L. D. Jacobson, J. Phys. Chem. A **115**, 14470 (2011).

[70] J. R. Casey, R. E. Larsen, and B. J. Schwartz, Proc. Natl. Acad. Sci. U.S.A. **110**, 2712, (2013).

[71] K. Toukan, and A. Rahman, Phys. Rev. B **31**, 2643 (1985).

[72] M. P. Allen, and D. J. Tildesley, *Computer Simulation of Liquids* (Clarendon, Oxford, 1987).

[73] P. Ayotte, and M. A. Johnson, J. Chem. Phys. **106**, 811 (1997).

[74] R. M. Stratt, and M. Cho, J. Chem. Phys. **100**, 6700 (1994).

[75] M. J. Bedard-Hearn, R. E. Larsen, and B. J. Schwartz, Phys. Rev. Lett. **97**, 130403 (2006).

[76] J. R. R. Verlet, A. E. Bragg, A. Kammrath, O. Cheshnovsky, and D. M. Neumark, Science **310**, 1769 (2005).

[77] L. Turi, W.-S. Sheu, and P. J. Rossky, Science **310**, 1769 (2005).

[78] B. B. Laird, and W. H. Thompson, J. Chem. Phys. **126**, 211104 (2007).

[79] F. Uhlig, O. Marsalek, and P. Jungwirth, J. Phys. Chem. Lett. **4**, 338 (2013).